Journal of Materials Chemistry A

Accepted Manuscript

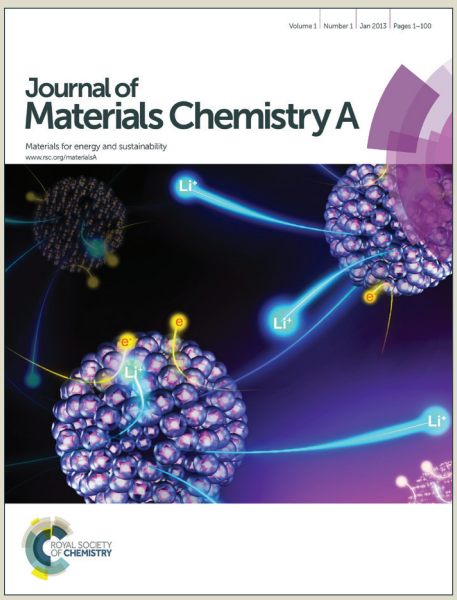

ROYAL SOCIETY OF CHEMISTRY

www.rsc.org/materialsA

Journal Name

RSCPublishing

ARTICLE

Interaction mechanism between functionalized protection layer and dissolved polysulfide for extended cycle life of lithium sulfur batteries

Wook Ahn[a*], Sung Nam Lim[b], Dong Un Lee[a], Kwang-Bum Kim[c], Zhongwei Chen[a], Sun-Hwa Yeon[d*]

Cite this: DOI: 10.1039/x0xx00000x

Received 00th January 2012,
Accepted 00th January 2012

DOI: 10.1039/x0xx00000x

www.rsc.org/

To improve the cycle life of Li-S rechargeable batteries, chemically dispersed nano carbon materials are usually employed as adsorbents and conductive matrices for the cathodic nano-sized sulfur materials. Herein, a new assembly for Li-S cells is developed by introducing montmorillonite (MMT) ceramic protective film to form an ion selective separator. The effect of the MMT-coated separator and the reaction mechanism between the MMT and polysulfides are characterized via Raman and Zeta Potential analyses. The utilization of the MMT coated separator enables the minimization of the shuttle effect by preventing the diffusion of the polysulfide. The best discharge capacity and cycle life are obtained with MMT coated separator in a sulfur-MWCNTs composite cathode, resulting in a discharge capacity of 1382 mAh g^{-1} at a current density of 100mA g^{-1} and 924 mAh g-1 after 200 cycles. The Li-S cell using the nano-size of sulfur-MWCNTs composite and the MMT-coated separator shows significantly excellent electrochemical performance.

Introduction

In recent years, lithium rechargeable batteries have required high theoretical power outputs and energy densities due to the development of high performance electric vehicles (EVs) and portable electric devices.[1-3] At present, among the commercially available rechargeable lithium-based batteries, lithium-ion batteries (LIBs) normally generate specific energies in the range of 100 to 200 Wh kg^{-1}.[4] Even though the cathode materials used in LIBs produce relatively low specific capacities, they are still in demand for high power and high energy density applications. To meet the requirements of both high power and high energy applications, a breakthrough in lithium based rechargeable batteries is much needed. In this regard, lithium-sulfur batteries have gained particular interest due to their high theoretical capacity (1675 mAh g^{-1}) and energy density (2600 Wh kg^{-1}). Additionally, lithium-sulfur batteries properly operates even in very low temperatures, again ideal for EV and portable electronics applications.[5] Furthermore, sulfur is relatively much cheaper material than intercalation materials, which makes lithium-sulfur batteries extremely cost effective. However, lithium-sulfur batteries still suffer from capacity diminution with advancing cycles and a low electronic conductivity of sulfur itself.[6,7] The capacity fading with advancing cycles results from the formation of highly soluble lithium polysulfide intermediates in non-aqueous electrolyte during the cycling process. For this battery system, the most significant solution is preventing the diffusion of lithium polysulfides.[8-10] Almost all published works studying lithium-sulfur batteries have focused on solving these problems in respect of electrode material, membrane, and electrolyte. In order to improve the capacity and prevent dissolution of lithium polysulfides, carbon-based sulfur composites obtained through various fabrication routes have previously been utilized as cathode materials, such as, the sulfur-impregnated carbon nanotubes or sulfur nanofiller composites constrained in porous carbon framework.[6,7,11-14] Also, in our previous work, a chemically dispersed sulfur-MWCNTs composite as a cathode material was synthesized via a simple direct precipitation route.[15,16] In another respect, various membrane treatments using some coating processes on separator have been utilized to enhance cycleability. The coating prepared by phase inversion using a montmorillonite (MMT) has been well known as a good method for improving physical and electrochemical stability in LIBs, and the high thermal and mechanical properties help to prohibit shortage caused by dendritic growth of lithium on the electrode surface.[17-21] In general, well-dispersed clay particles in a polymeric matrix can improve thermal and mechanical properties of films[22], and hydrophilic MMT can provide enhanced wettability of liquid electrolytes.[23] However, to the best of our knowledge, the MMT coating have never been implemented in a Li-S battery system as a protective layer for

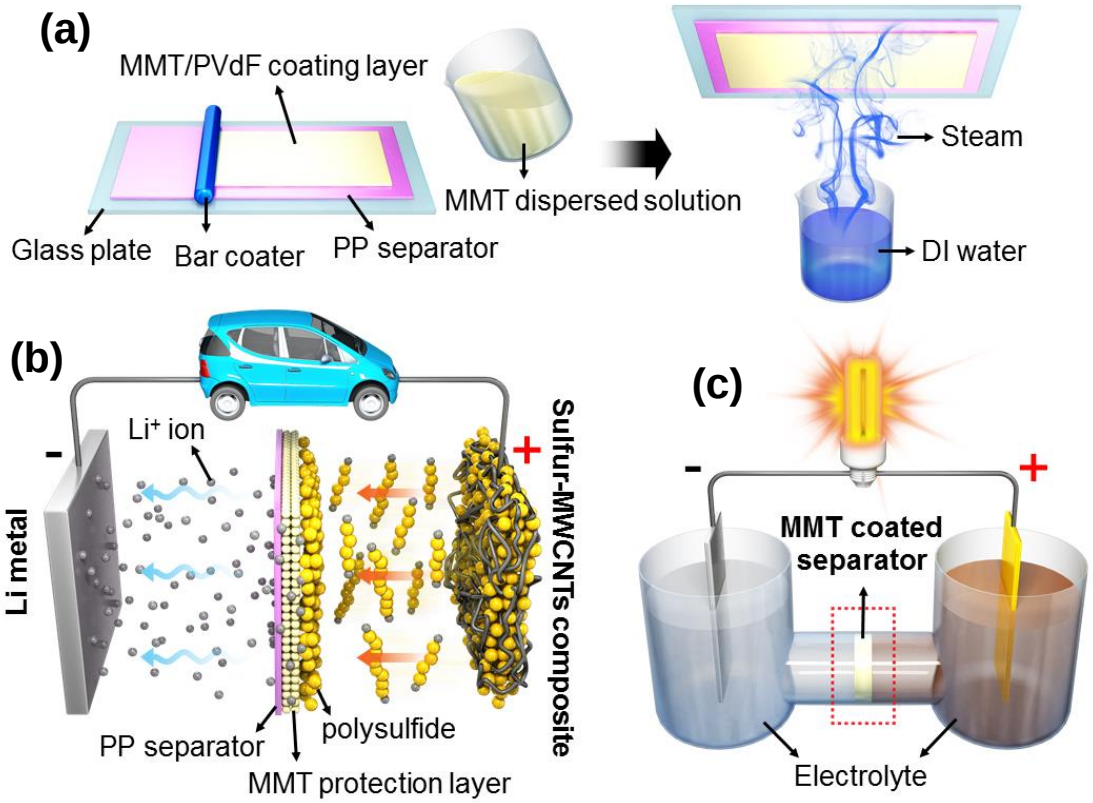

Fig. 1 Schematic configuration of preparation procedure of MMT coated separator (a), theoretical mechanism of Li-S cell using MMT coated separator (b) and electrochemical cell for Raman analysis (c).

preventing the diffusion of lithium polysulfiedes. In this work, we have demonstrated excellent electrochemical properties, for the first time, by using MMT-coated onto a protective PP layer as an effective separator for preventing lithium polysulfides in a Li-S battery system. Simultaneously, the sulfur-MWCNTs composite have been used as cathode[15,16] and invested by Raman to examine the behavior of lithium polysulfide within the lithium sulfur cell during the charge-discharge processes. The manufacturing process for MMT coated separator and electrochemical cell for Raman study are presented in Figure 1.

Experimental section

Preparation of sulfur/MWCNTs composite and MMT coated separator

The synthesis of the sulfur-MWCNTs composite and the manufacturing procedure of the MMT coated separator are presented in Figure 1. A detailed preparation of the sulfur-MWCNTs composite using the direct precipitation method has been described previously in "Direct precipitation method".[16] In order to synthesize the sulfur-MWCNTs composite, the MWCNTs were dispersed in a 0.1 mol $Na_2S_2O_3$ solution with vigorous mixing. Then the solution was sonicated for 2 h, after which a 0.1 mol H_2SO_4 solution was added dropwise into this solution at a rate of 10 mL min^{-1}. In order to adjust the amount of precipitated sulfur (3.88 g) in the composite, the amount of MWCNTs added to the solution was 0.97 g producing a weight ratio in the final composite (sulfur:MWCNTs) of approximately 80:20.

The preparation of the MMT (montmorillonite: Sigma-Aldrich, K 10) coated separator was conducted using a simple casting process and phase inversion of MMT clays using distilled water. The procedure is as follows: 1.5 g PVdF-HFP co-polymer (Kynar 2801) was used as a binder in a mixed solution of 7 g N-methyl propylene and 5 g of acetone, using a paste mixer. Then 1.5 g of MMT powder was gradually added into the solution, and stirred using a planetary mixer for 4 hours at room temperature. After vigorous mixing, the mixture was coated on a separator (Celgard 3501) to a 25 μm thickness using a bar-coater. The coated separator was then dried at room temperature for 1 hour. In order to conduct the phase inversion of the MMT clay, it was exposed to steam from boiling distilled water for 10 minutes. After the phase inversion, the MMT-coated separator was dried in an oven at 60 ^oC for 24 hours under vacuum. The final loading of MMT-copolymer protection layer on the PP separator was 1.65 mg/cm^2 (MMT: 0.825 mg/cm^2, PVdF-co-HFP: 0.825mg/cm^2.

Characterization: physical and electrochemical properties

To confirm the amount of sulfur content in the sulfur/MWCNT

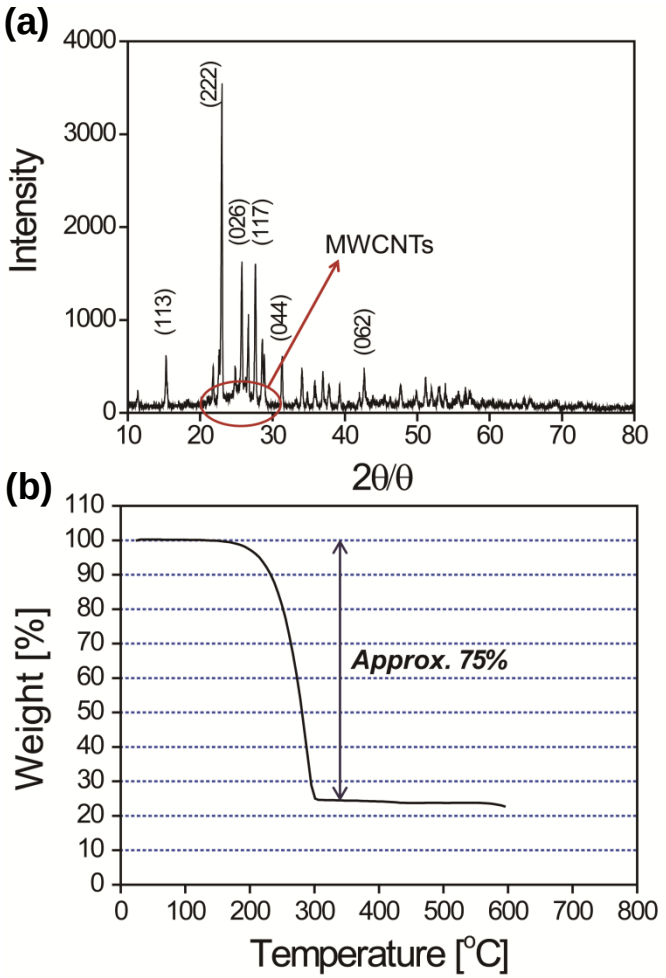

Fig. 2 XRD pattern (a) and TGA result (b) of sulfur/MWCNT composite.

composite, thermogravimetric analysis (TGA/SDTA851^e-METTLER) was performed across a temperature range of 25 – 600 ^oC with a 5 ^oC/min heating rate in air. For the structural analysis, X-ray diffraction of the phases was carried out using aHPC-2500 XRD (Gogaku) with Cu Kα radiation (λ = 1.5405Å) in the 2θ range of 10 – 80^o with 0.02^o intervals, at a 2^o/min scanning rate. The morphology of the synthesized sulfur/MWCNT composite and the MMT-coated separator were analyzed using a scanning electron microscope (SEM; S4700, Hitachi). In order to quantify the lithium polysulfide in the electrolyte and on the side of the cathode, Raman spectrometry (DXR Raman Microscope, Thermo Fisher Scientific) with a frequency diode laser at 532 nm was used. The electrochemical cell for Raman analysis was evaluated and the schematic diagram is presented in Figure 1. After manufacturing an electrolyte test cell, the charge-discharge across 5 cycles was examined. In order to verify the driving force between the MMT and the polysulfide, the Zeta Potential (ELS-8000, Otasuka Electronics Co.) of MMT was measured.

For electrochemical testing, the cathode electrodes were prepared by mixing 20 wt.% PVdF-HFP co-polymer (Kynar 2801)- as binder and 80 wt.% of the sulfur-MWCNT composite in N-methyl-2-pyrrolidone (NMP), then this slurry was mixed

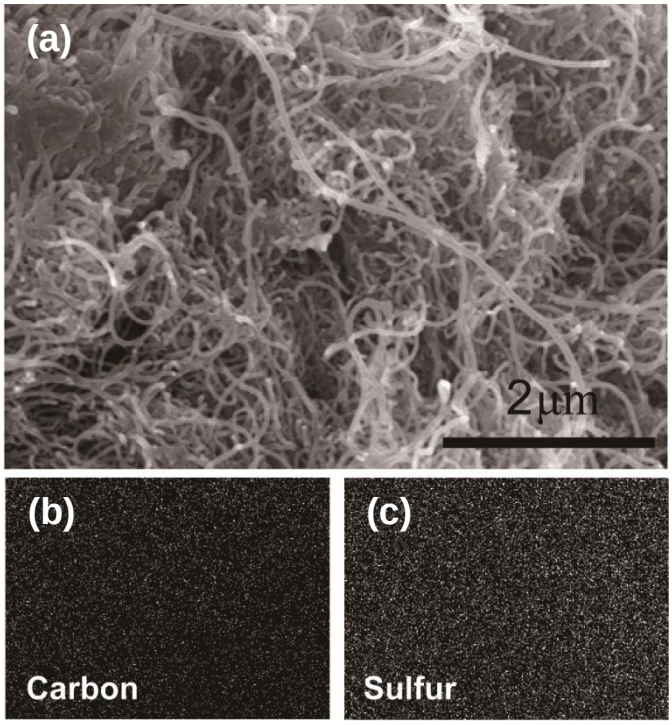

Fig. 3 SEM image (a) and EDS mapping result (b:carbon, c:sulfur) obtained from Sulfur-MWCNTs composite.

using a planetary mixer with a zirconia ball for 3 hrs to achieve a uniform mix. This slurry was then coated on Al foil (20 μm) to a 60 μm thickness using a doctor blade to form the cathode. The electrode was pressed using a twin roller and dried at 70 ^oC under a vacuum. The final thickness of the cathode material on the Al foil was 50 μm, and the sulfur loading was 0.7 mg/cm^2. CR2032 coin-type cells were assembled using 1.0 M $LiCF_3SO_3$ and 0.2 M $LiNO_3$ in a mixture of tetra (ethylene glycol) dimethyl ether (TEGDME)/1,3-dioxolane (DOL) (50:50 vol.%) as an electrolyte. Lithium foil was used as the counter electrode. The electrode was size 14Ø and 80μl of the electrolyte was injected. Both an uncoated and a MMT-coated separator as separator were used in the test cells. In order to verify the influence of the MMT-coated separator, the side coated with the MMT was placed facing the cathode. The entire procedure for the coin cell assembly was performed in an argon (Ar) filled glove box. Fabricated coin cells were aged for 2 hr at room temperature in an oven. Then the charge and discharge cycles were carried out (MACCOR 4000 SERIES) at a current density of 100 mA g^{-1} (based on the sulfur) with a voltage range between 1.6-2.8V at room temperature.

Results and Discussion

Figure 2 (a) presents the XRD pattern of the sulfur-MWCNTs composite, and all the measured peak positions correspond to the sulfur octatomic molecules with S_8 which is highly polymorphic and forms orthorhombic phase (α-S_8) with the space group Fddd (JCPDS 83-2283). Also, there are no peaks related to impurities except for the slightly broadened XRD

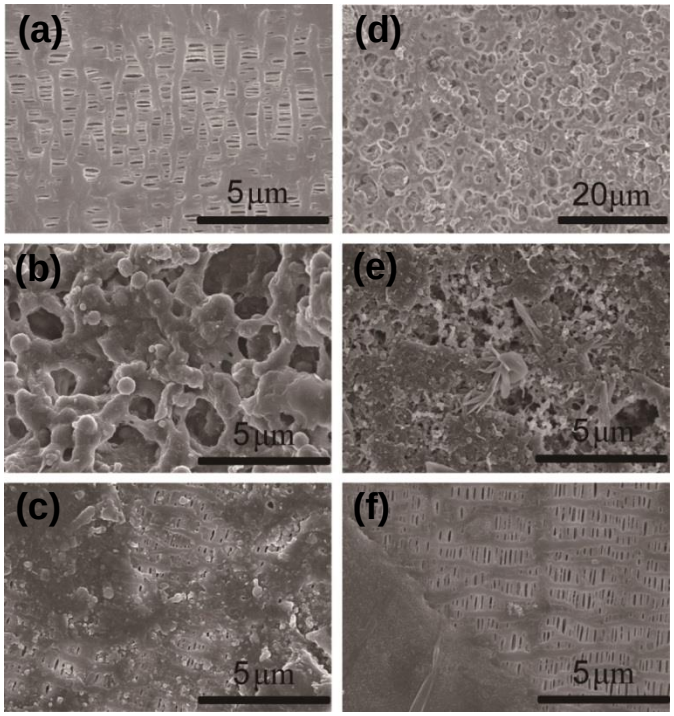

Fig. 4 SEM images of as-received separator: before electrochemical test (a), front side (b) and back side (C) after test; MMT-coated separator: before electrochemical test (d), front side (e) and back side (f) after cell test.

peak around ca. 26° due to the well-dispersed MWCNTs, indicative of homogeneity of the composite obtained by the direct precipitation method. Figure 2 (b) shows the TGA-DTA results of the mixed precursor powder from 25 °C to 600 °C under a nitrogen atmosphere. There are only one weight loss stages apparent in the TGA curve. The abrupt weight loss in 25 °C ~ 350 °C temperature range reflects the sulfur decomposition and the weight loss is approximately 75 wt.%, in accordance with our previous work.[16]

Figure 3 (a) shows the SEM image of synthesized sulfur-MWCNTs. It is apparent in Figure 3 (a) that the MWCNTs and the precipitated sulfur are intertwined, implying that the precipitated sulfur is dispersed uniformly. The MWCNTs uniformity in the composite is shown by EDS maps presented in Figure 3 (b) and (c), with the bright spots indicating the presence of the elements carbon and sulfur, respectively. The EDS mapping results demonstrate that the sulfur is well distributed throughout the entire surface of the MWCNTs though the direct precipitation method.

Figure 4 (a) and (d) show the SEM images of as-received PP separator and MMT-coated separator before electrochemical test, respectively. From Figure 4 (d), it is clear that the MMT particles are well dispersed on the separator surface with excellent uniformity. The used cathode-side and anode-side after electrochemical tests are presented in Figure 4 (b) and (c) in as-received separator and Figure 4 (e) and (f) in MMT coated separator, respectively. It could be verified that the dissolved polysulfide is covered on the surface of cathode-side of the two separators (Figure 4 (b) and (e)). However very interestingly,

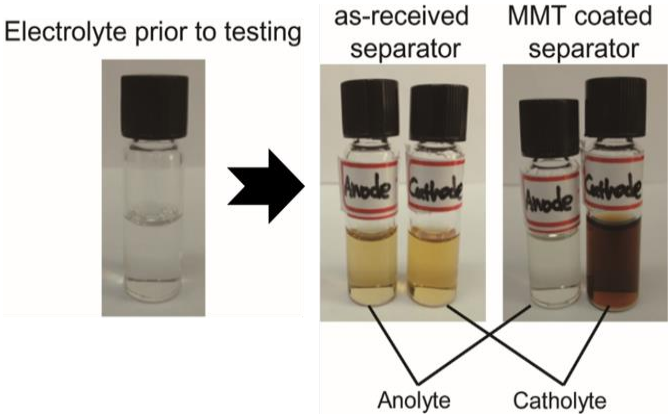

Fig. 5 The colour change comparison of the catholyte and the anolyte employing the as-received separator and MMT-coated separator.

the anode-side (Figure 4(c)) of as-received separator is also covered with the diffused polysulfide, whereas that of the MMT-coated separator (Figure 4(f)) is still pristine and the pores for lithium ion transportation are sustained. Therefore, SEM observation strongly suggests that a simple MMT coating is extremely effective in preventing the diffusion of polysulfide through the separator. When sulfur molecules react with the lithium ions, they become soluble lithium polysulfides (when using organic electrolytes) which cause the problem of rapid capacity decay in lithium sulfur batteries.[24-26] When this occurs, the color of the organic electrolyte changes from white to brown or dark brown. It is known that the dissolved lithium polysulfides in the electrolyte lead to the shuttle mechanism.[6-8] Once the lithium polysulfide is dissolved, it can easily diffuse to the anode side, suppressing the reduction of lithium ions to lithium metal. This irregular reaction causes the infinite charge and decreases capacity.[26,27] To restrict the shuttle mechanism, the MMT coated layer on the separator prevents the diffusion of polysulfide anions through the separator. In order to evaluate the function of preservation, both the MMT-coated and the as-received separators (Celgard 3501) are compared after electrochemical testing. Figure 5 shows the color comparison for the catholyte and the anolyte after using the two separators. The tested cell for the separation of the electrolyte after testing have been prepared as shown in Figure 1(c). In the case of the as-received separator, the catholyte and anolyte on both sides of the electrode changed to a thin dark brown color. However, while the anolyte of the MMT-coated separator remained unchanged, the catholyte of that was changed to heavy dark brown. This is clear visual evidence that the MMT-coating layer prevents lithium polysulfide diffusion to the anode.

Figure 6 (a)-(c) shows the optical microscope images of the MMT coated separator prior to testing (a) and the cathode side (b) and anode side (c) after testing. The surface of the cathode side (b) after cycling shows the accumulated lithium polysulfide. Also, it appears that the surface colour of anode side has changed to silver, resulting from the lithium sulfides accumulated on the surface and/or in the separator pores. The optical microscope images of the as-received separator before (d) and after testing (e)-(f) are presented in Figure 6,

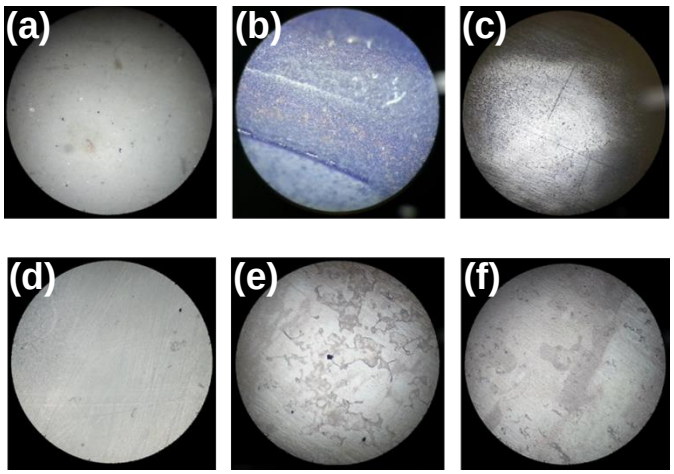

Fig. 6 Optical images of separators using MMT coated separator (a: prior to testing, b: cathode side after testing, c: anode side after testing); using as-received separator (d: prior to testing, e: cathode side after testing, f: anode side after testing).

respectively. The surfaces of both sides of the PP separator have changed to a partially stained color, indicating that the dissolved lithium polysulfide has diffused to the anode side. From these microscope images and the color changes observed in Figure 5, it is evident that the dissolved lithium polysulfide is accumulated only on the MMT-coated cathode side during the electrochemical reduction and oxidation cycles, preventing polysulfide diffusion to the anode side thereby suppressing the shuttle mechanism caused by lithium polysulfide formation.

To further investigate the effectiveness of the MMT coated separator, Raman spectroscopy has been utilized to study various battery components. Figure 7 (a) and (b) show comparative Raman analyses of the catholyte and the anolyte before and after testing for the electrochemical cell (Figure 1(c)) containing the as-received separator (Figure 7 (a)) and MMT-coated separator (Figure 7 (b)), respectively. The electrolyte prior to testing shows pronounced peaks at 314, 348, 759, 942, 1043, 1231, 1477, 2765, 2891 and 2955 cm^{-1}. The intensity of these peaks decreased for both sides of the as-received separator after testing. After testing the broad peaks, representative of lithium polysulfide, appeared at approximately 2200 and 2800 cm^{-1}. The strong peaks at 2765, 2891 and 2955 cm^{-1} indicated in electrolyte before the testing disappeared after that. At the MMT-coated separator sample (in Figure 7 (b)), while the strong peaks at 2765, 2891 and 2955 cm^{-1} in catholyte have also disappeared, the broad week peaks of lithium polysulfide (2436 and 2552 cm^{-1}) are revealed. However, the electrolyte on the anode side of the MMT-coated separator after the cell test remains unchanged, further making the MMT coated layer suppress the lithium polysulfide diffusion to the anode side.

Figure 8 presents the Raman spectra obtained from pure sulfur, sulfur-MWCNTs composite and Li_2S (theoretically the material left after full discharge). The pristine sulfur shows strong Raman modes of sulfur at 151, 217 and 471 cm^{-1}. The Raman spectra of the synthesized sulfur-MWCNTs composite shows

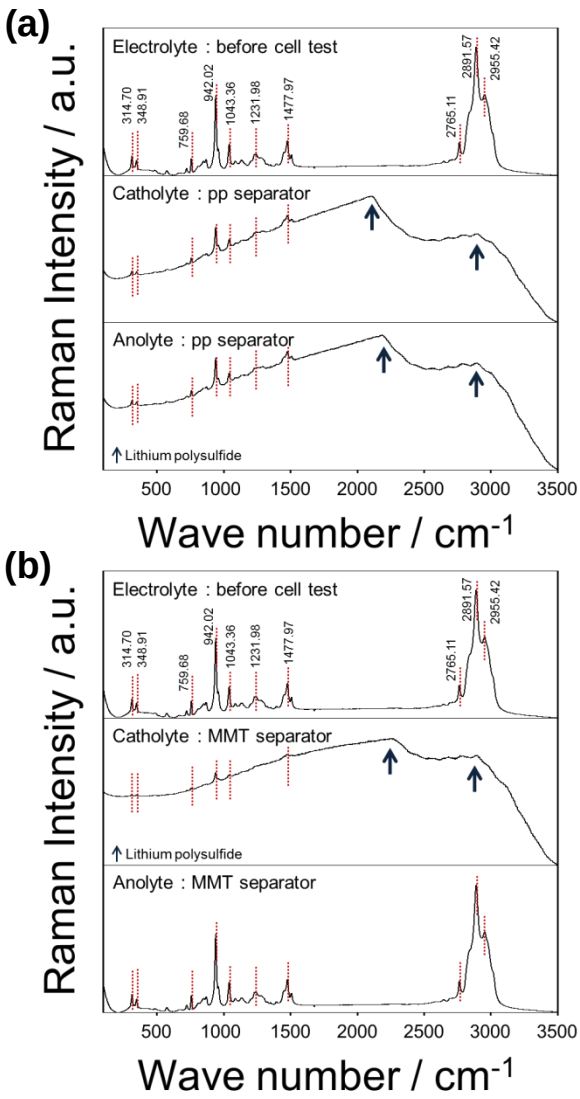

Fig. 7 Raman study results for electrolyte using (a) PP separator before electrochemical test and after test; (b) MMT-coated separator before electrochemical test and after test

the same Raman modes of sulfur as well as the G, D and 2D peaks of MWCNTs. The fully discharged electrode sample shows strong main peaks of 372 and 481 cm^{-1} and weak peaks at 2436 and 2552 cm^{-1}, which correspond to lithium sulfides (strong Raman mode) and lithium polysulfide (weak Raman mode) produced during Li-S reaction, respectively.[28] To identify the interaction mechanism between the MMT and polysulfide anions during the charge-discharge advanced, the Zeta potential is conducted using reference solvent. The Zeta Potential results, MMT dispersed in deionized water (DI) and in 2-propanol gave respective values of -96.18 mV and -63.34 mV (Figure 9), confirming the driving force between the MMT and polysulfide anions, since polysulfide exists as an anion in the organic electrolyte and the MMT is also negatively charged. From these intrinsic characteristics, the repulsive forces between the MMT and polysulfide anion is interacted, leading to the stable performance. If the MMT has positive charge in

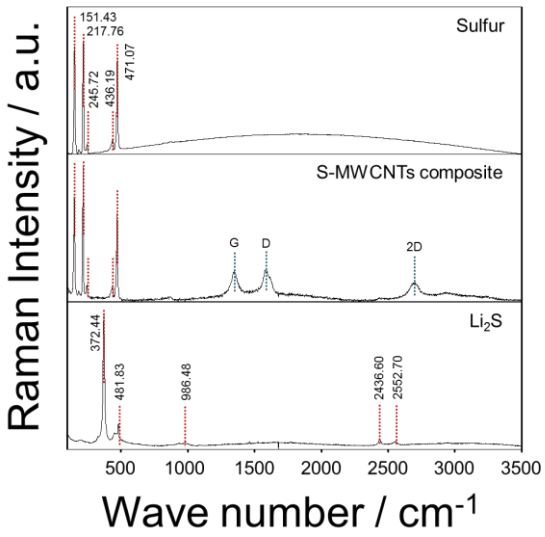

Fig. 8 Raman study result of materials (sulfur, sulfur-MWCNTs composite and Li_2S).

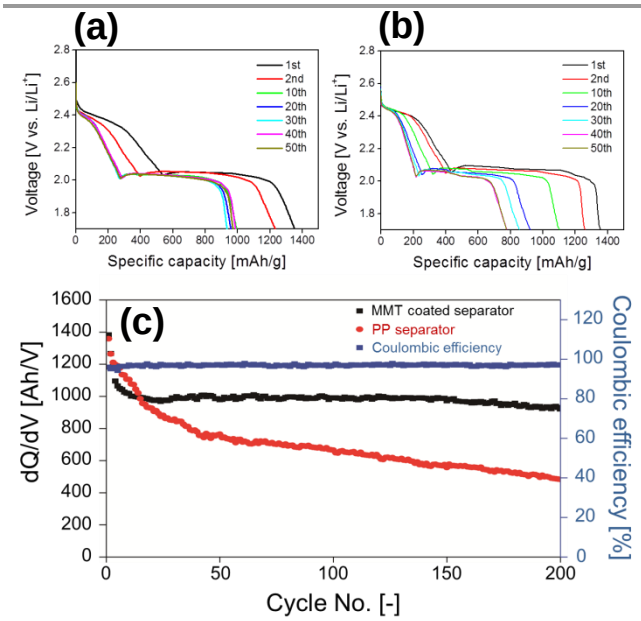

Fig. 10 Discharge curves of LiS cells using MMT-coated separator (a) and as-received separator (b); comparison of cycle performance using as-received separator and MMT-coated separator.

electrolyte, the dissolved polysulfide is adsorbed in MMT. Then, the concentration of polysulfide would be getting lower in electrolyte, leading to the additional dissolution of active material to adjust the intrinsic solubility of polysulfide in organic electrolyte. Therefore, the dissolved polysulfide is blocked from diffusing through the separator due to the repulsive ionic forces, proving the reaction mechanism of the MMT-coated separator when used as a protection layer. Based on this result, it is assumed that the bond of high ordered

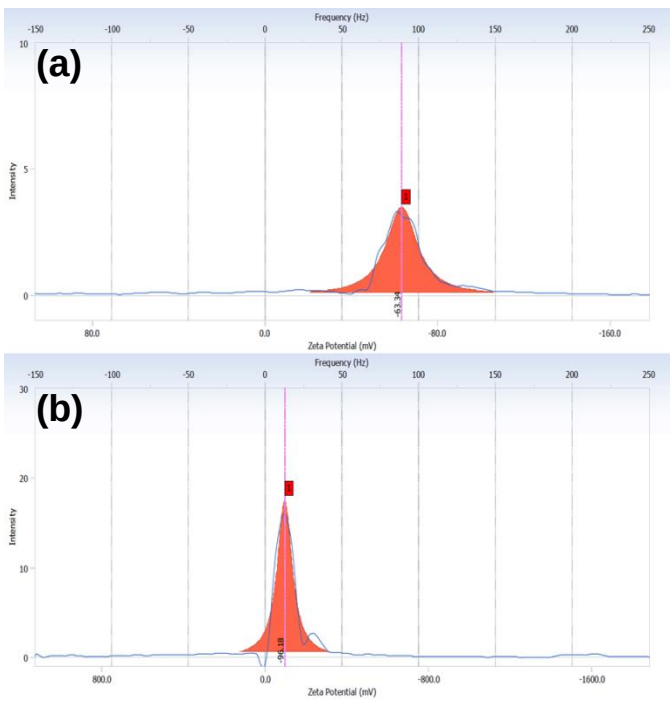

Fig. 9 Zeta potential result of MMT powder (a: dispersed in DI, b: dispersed in 2-propanol).

lithium polysulfide is broken by repulsive interaction between MMT anion and polysulfide anion during the charge process, leading to the reduction of metallic lithium on the anode. Figure 10 displays the discharge profiles (Figure 10 (a-b)) and cycleability (Figure 10 (c)) determined from the lithium sulfur cells in the MMT-coated separator and as-received separator. The initial discharge capacity was approximately 1380 mAh g^{-1} for both cells. However, only after 10 cycles, the capacity is significantly diminished for the cell using the as-received separator. The discharge capacities obtained from the as-received or MMT-coated separator after 200 cycles are 476 mAh g^{-1} and 924 mAh g^{-1} respectively. For initial cycles, the decrease rate for the as-received separator cell is relatively small. However, after 5 cycles, the test cell with MMT coated separator maintains the capacity in the 1000 mAh g^{-1} range. The coulombic efficiency of the cell using MMT-coated separator shows *ca.* 97% after 200cycles. The discharge profiles of all cells show commonly observed two plateaus, at approximately 2.4 and 2.1 V_{Li/Li^+}. These two plateaus indicate lithium polysulfide formation while the discharge process is advanced. It is accepted[29] that the first plateau is the transformation of elemental sulfur to lithium polysulfide. From this result, it is clearly shown that the MMT-coated separator enhances the electrochemical performance of the cell. The MMT-coating layer enhances the cycleability by suppressing the diffusion of lithium polysulfide to the anode side. These results are in agreement with the Raman study.

Conclusion

In summary, a montmorillonite (MMT) coated separator was successfully manufactured using phase inversion method for lithium sulfur batteries. As a cathode material, a sulfur-

MWCNTs composite was prepared through a simple methode, consisting of 75 wt.% sulfur and 25 wt.% MWCNTs. The SEM results confirmed that the MMT was homogeneously coated on the bare pp separator and that the sulfur was well dispersed on the surface of the MWCNTs. In the Raman study and Zeta Potential analysis, it is confirmed that the MMT layer coated on a bare PP separator can suppress the dissolved sulfur diffusion to the anode side by repulsive electrostatic force between the polysulfide and the MMT. The electrochemical analysis showed that the MMT-coated separator make possible to maintain the discharge capacity of 924 mAh g^{-1} at 200 cycles from the initial capacity of 1380 mAh g^{-1}. Therefore, the MMT coating on a bare separator is a promising protection layer to improve the electrochemical capacity and cycleablity by suppressing lithium polysulfide diffusion to anode side in Li-S battery.

Acknowledgements

This work was supported by the Next Generation Military Battery Research Center program of The Defense Acquisition Program Administration and Agency for Defense Development.

Notes and references

[a] *Department of Chemical Engineering, University of Waterloo, 200 University Ave W. Waterloo, ON, N2L3G1, Canada. Fax: +1-519-888-4347; Tel: +1-519-888-4567 Ext. 31614; E-mail: wahn@uwaterloo.ca*
[b] *Department of Chemical & Biomolecular Engineering, Korea Advanced Institute of Science and Technology, 291 Daehak-ro, Yuseong-gu, Daejeon 305-701, Korea.*
[c] *Department of Materials Science & Engineering, Yonsei University, 50 Yonsei-ro, Seodaemun-Gu, Seoul, 120-749, Korea*
[d] *Korea Institute of Energy Research, 152 Gajeong-ro, Yuseong-Gu, Daejeon, 305-343, Korea. Fax: +82-42-860-3133; Tel: +82-42-860-3763; E-mail: ys93@kier.re.kr*

1. P. Gibot, M. Casas-Cabanas, L. Laffont, S. Levasseur, P. Carlach, S. Hamelet, J.-M. Tarascon, C. Masquelier, *Nature materials* 2008, **7**, 741-747.
2. B. Zhang, G. Chen, Y. Liang, P. Xu, *Solid State Ionics* 2009, **180**, 398-404.
3. J.-H. Cho, J.-H. Park, M.-H. Lee, H.-K. Song, S.-Y. Lee, *Energy & Environmental Science* 2012, **5**, 7124-7131.
4. T. Ohzuku, R. J. Brodd, *Journal of Power Sources* 2007, **174**, 449-456.
5. D. Marmorstein, T. Yu, K. Striebel, F. McLarnon, J. Hou, E. Cairns, *Journal of Power Sources* 2000, **89**, 219-226.
6. N. Jayaprakash, J. Shen, S. S. Moganty, A. Corona, L. A. Archer, *Angewandte Chemie* 2011, **123**, 6026-6030.
7. X. Ji, K. T. Lee, L. F. Nazar, *Nature materials* 2009, **8**, 500-506.
8. H. Wang, Y. Yang, Y. Liang, J. T. Robinson, Y. Li, A. Jackson, Y. Cui, H. Dai, *Nano letters* 2011, **11**, 2644-2647.
9. H. Yamin, A. Gorenshtein, J. Penciner, Y. Sternberg, E. Peled, *Journal of the Electrochemical Society* 1988, **135**, 1045-1048.
10. J. Shim, K. A. Striebel, E. J. Cairns, *Journal of the Electrochemical Society* 2002, **149**, A1321-A1325.
11. J. Wang, J. Yang, J. Xie, N. Xu, Y. Li, *Electrochemistry Communications* 2002, **4**, 499-502.
12. C. Liang, N. J. Dudney, J. Y. Howe, *Chemistry of Materials* 2009, **21**, 4724-4730.
13. J. Wang, S. Chew, Z. Zhao, S. Ashraf, D. Wexler, J. Chen, S. Ng, S. Chou, H. Liu, *Carbon* 2008, **46**, 229-235.
14. J. Guo, Y. Xu, C. Wang, *Nano letters* 2011, **11**, 4288-4294.
15. R. G. Chaudhuri, S. Paria, *Journal of colloid and interface science* 2010, **343**, 439-446.
16. W. Ahn, K.-B. Kim, K.-N. Jung, K.-H. Shin, C.-S. Jin, *Journal of Power Sources* 2012, **202**, 394-399.
17. G. G. Kumar, K. S. Nahm, R. N. Elizabeth, *Journal of Membrane Science* 2008, **325**, 117-124.
18. M. Wang, F. Zhao, Z. Guo, S. Dong, *Electrochimica acta* 2004, **49**, 3595-3602.
19. M. J. Koh, H. Y. Hwang, D. J. Kim, H. J. Kim, Y. T. Hong, S. Y. Nam, *Journal of Materials Science & Technology* 2010, **26**, 633-638.
20. M. Raja, T. P. Kumar, G. Sanjeev, L. Zolin, C. Gerbaldi, A. M. Stephan, *Ionics* 2014, **20**, 943-948
21. J. Nunes-Pereira, A. C. Lopes, C. M. Costa, R. Leones, M. M. Silva, S. Lanceros-Mendez, *Electroanalysis* 2012, **24(11)**, 2147-2156
22. J. H. Chang, Y. U. An, *Journal of Polymer Science Part B: Polymer Physics* 2002, **40**, 670-677.
23. Y.-P. Wang, X.-H. Gao, R.-M. Wang, H.-G. Liu, C. Yang, Y.-B. Xiong, *Reactive and Functional Polymers* 2008, **68**, 1170-1177.
24. Z. W. Seh, W. Li, J. J. Cha, G. Zheng, Y. Yang, M. T. McDowell, P.-C. Hsu, Y. Cui, *Nature communications* 2013, **4**, 1331.
25. Y. Yang, G. Yu, J. J. Cha, H. Wu, M. Vosgueritchian, Y. Yao, Z. Bao, Y. Cui, *Acs Nano* 2011, **5**, 9187-9193.
26. G. Zheng, Y. Yang, J. J. Cha, S. S. Hong, Y. Cui, *Nano letters* 2011, **11**, 4462-4467.
27. S. Dörfler, M. Hagen, H. Althues, J. Tübke, S. Kaskel, M. J. Hoffmann, *Chemical Communications* 2012, **48**, 4097-4099.
28. J.-T. Yeon, J.-Y. Jang, J.-G. Han, J. Cho, K. T. Lee, N.-S. Choi, *Journal of The Electrochemical Society* 2012, **159**, A1308-A1314.
29. P. G. Bruce, S. A. Freunberger, L. J. Hardwick, J.-M. Tarascon, *Nature materials* 2012, **11**, 19-29.